Correlation of Proton Release and Electrochromic Shifts of the Optical Spectrum Due to Oxidation of Tyrosine in Reaction Centers from *Rhodobacter sphaeroides*†

L. Kálmán,‡,§ R. LoBrutto,|| A. J. Narváez,‡ J. C. Williams,‡ and J. P. Allen*,‡

Departments of Chemistry and Biochemistry and of Plant Biology, Arizona State University, Tempe, Arizona 85287

Received June 5, 2003; Revised Manuscript Received September 15, 2003

ABSTRACT: Reaction centers from the Y_{L167} mutant of *Rhodobacter sphaeroides*, containing a highly oxidizing bacteriochlorophyll dimer and a tyrosine residue substituted at Phe L167, were compared to reaction centers from the Y_M mutant, with a tyrosine at M164, and a quadruple mutant containing a highly oxidizing dimer but no nearby tyrosine residue. Distinctive features in the light-induced optical and EPR spectra showed that the oxidized bacteriochlorophyll dimer was reduced by Tyr L167 in the Y_{L167} mutant, resulting in a tyrosyl radical, as has been found for Tyr M164 in the Y_M mutant. In the Y_{L167} mutant, the net proton uptake after formation of the tyrosyl radical and the reduced primary quinone ranged from +0.1 to +0.3 H^+/reaction center between pH 6 and pH 10, with a dependence that is similar to the quadruple mutant but different than the large proton release observed in the Y_M mutant. In the light-induced absorption spectrum in the 700−1000 nm region, the Y_{L167} mutant exhibited unique changes that can be assigned as arising primarily from an approximately 30 nm blue shift of the dimer absorption band. The optical signals in the Y_{L167} mutant were pH dependent, with a pK_a value of approximately 8.7, indicating that the tyrosyl radical is stabilized at high pH. The results are modeled by assuming that the phenolic proton of Tyr L167 is trapped in the protein after oxidation of the tyrosine, resulting in electrostatic interactions with the tetrapyrroles and nearby residues.

In photosynthetic bacteria, energy conversion takes place in a membrane-bound complex called the reaction center. Light absorption results in the transfer of an electron from the primary electron donor, P,[1] a bacteriochlorophyll dimer, through intermediates to the primary quinone, Q_A, and then to the secondary quinone, Q_B (*1*, *2*). The subsequent absorption of a second photon results in the double reduction of Q_B in a reaction that is coupled to the uptake of two protons. When electron transfer from Q_A^- to Q_B is blocked, the state $P^+Q_A^-$ is stable for approximately 100 ms in wild type, and a substoichiometric proton release due to P^+ and substoichiometric proton uptake due to Q_A^- are observed (*3*, *4*).

The structures of the bacterial reaction center and photosystem II are homologous despite significant differences in their function (*5*, *6*). The two protein complexes have a core structural motif consisting of two branches of cofactors enveloped by five transmembrane helices from two subunits that are related by an approximate 2-fold symmetry axis. The oxidized donor of the bacterial reaction center is reduced by a water-soluble cytochrome c_2 while the secondary donor for the oxidized donor of photosystem II is a redox-active tyrosine Y_Z (*7*−*10*). The chemical ability to oxidize tyrosines requires a high midpoint potential, such as the ∼1 V potential of the chlorophyll donor of photosystem II, compared to the ∼0.5 V potential for P in bacterial reaction centers. The P/P^+ midpoint potential in reaction centers from *Rhodobacter sphaeroides* can be increased to at least 0.8 V in a mutant that contains the substitutions Leu L131 to His, Leu M160 to His, Phe M197 to His, and Tyr M210 to Trp (*11*). This quadruple mutant has the same spectral characteristics as wild type, except for a significant decrease in spectral amplitudes due to the low quantum yield of 5−10% (*11*). An additional mutation is included in the Y_M mutant, in which a tyrosine is placed in the highly oxidizing reaction centers at M164, an analogous position to the redox-active tyrosines, Y_Z and Y_D, of photosystem II. In the Y_M mutant, $P^+Q_A^-$ is formed upon exposure to light, and subsequently Tyr M164 becomes oxidized by P^+ to an extent that is highly dependent upon the pH. Similar results are seen when a tyrosine is substituted at L135.

The light-induced radical in the Y_M mutant is similar to the Y_Z and Y_D tyrosyl radicals in that all are neutral radicals resulting from the phenolic proton of the tyrosine being released during electron transfer. Substantial efforts have been made to identify the details of the electron−proton-coupled reactions in oxygen evolution, with a focus on the fate of the phenolic proton of Y_Z, that is, whether it is released to the lumen or trapped within the protein (*12*−*14*). Proton release into the bulk solution upon the oxidation of Tyr M164 in the Y_M mutant could be described equally well by a model in which the phenolic proton goes to the bulk solution via a hydrogen-bonded network of protonatable amino acid residues or by a model in which the released

† This work was supported by Grant MCB 0131764 from the NSF.

* To whom correspondence should be addressed: phone, 480-965-8241; fax, 480-965-2747; e-mail, jallen@asu.edu.

‡ Department of Chemistry and Biochemistry, Arizona State University.

§ Permanent address: Department of Biophysics, University of Szeged, Egyetem u.2, H-6722 Szeged, Hungary.

|| Department of Plant Biology, Arizona State University.

[1] Abbreviations: P, primary electron donor; Q_A, primary quinone; Q_B, secondary quinone.

10.1021/bi034970l CCC: $25.00
Published on Web 10/24/2003

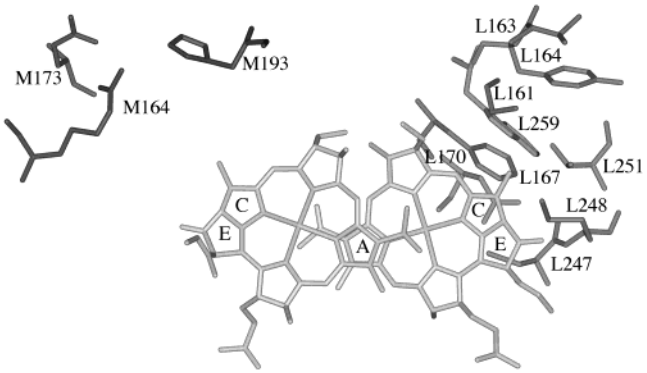

FIGURE 1: Structural view of the wild-type reaction center showing the bacteriochlorophyll dimer and residues Gly L161, Thr L163, Tyr L164, Phe L167, Asn L170, Cys L247, Met L248, Thr L251, Trp L259, Arg M164, Glu M173, and His M193. In the Y_{L167} mutant, Phe L167, located approximately 5 Å from the E ring on the L side of P, is replaced with Tyr. The nearest residues to the hydroxyl group of Tyr L167 in the Y_{L167} mutant, assuming a similar position to Phe L167, would be Cys L247, Met L248, and Thr L251, all of which are buried in the protein. Other residues near the ring of L167 include Gly L161, Tyr L164, Asn L170, and Trp L259. No obvious proton pathway or hydrogen-bonding network connects L167 to residue Thr L163, which is exposed to the surface of the protein. In the Y_M mutant, Arg M164, located approximately 10 Å from P, is substituted with Tyr. The putative proton acceptor for Tyr M164 in the Y_M mutant is His M193, and these residues likely interact with Glu M173, which is located on the surface of the protein. The axis of the Q_y transition of each bacteriochlorophyll is through the A−C rings, so for P, the Q_y transition is approximately along the two C rings.

protons are the result of a change in electrostatic interactions (*15*). In the latter case, the trapped positive charge induces shifts in the pK_a values of the surface residues, and these residues release the protons to the solution (*12*).

We describe here the characteristics of another mutant, named Y_{L167}, in which a tyrosine residue is substituted for Phe L167 in a reaction center that also has the four mutations (Leu L131 to His, Leu M160 to His, Phe M197 to His, and Tyr M210 to Trp) that produce a highly oxidizing bacteriochlorophyll dimer. The tyrosine in the Y_{L167} mutant is in a hydrophobic region of the protein and is much closer to P, at 5 Å, than Tyr M164, which is 10 Å from P, in the previously described Y_M mutant (Figure 1). The light-induced optical and EPR spectra and the stoichiometry of the light-induced proton uptake and release were measured in the Y_{L167} mutant for a range of pH values. The resulting pK_a values and stoichiometry of the protonational changes associated with tyrosine oxidation are discussed in terms of different possible mechanisms of proton release.

MATERIALS AND METHODS

Construction of Mutants and Protein Isolation. The quadruple mutant (Leu L131 to His, Leu M160 to His, Phe M197 to His, and Tyr M210 to Trp) and the Y_M mutant (Leu L131 to His, Leu M160 to His, Arg M164 to Tyr, Phe M197 to His, and Tyr M210 to Trp) have been previously described (*11*). The Y_{L167} mutant (Leu L131 to His, Phe L167 to Tyr, Leu M160 to His, Phe M197 to His, and Tyr M210 to Trp) was constructed by oligonucleotide-directed mutagenesis and by manipulation of restriction fragments as previously described (*16*). Cells were grown semiaerobically, and the reaction centers were prepared as described earlier, except that the nonionic detergent Triton X-100 was used for the ion-exchange chromatography step instead of the ionic detergent LDAO (*17*). After preparation, the reaction centers were stored in 15 mM Tris-HCl, pH 8.0, 0.05% Triton X-100, and 1 mM EDTA. For the proton uptake measurements, the Tris-HCl and the EDTA were removed by ion-exchange chromatography followed by dialysis against 0.05% Triton X-100 and 100 mM NaCl.

Measurement of Absorption Changes. Optical absorption changes were measured using a Cary 5 spectrophotometer (Varian). Excitation of the samples was achieved with short (<10 s) nonsaturating continuous light illumination, using an Oriel tungsten lamp with an interference filter (860 ± 15 nm). To avoid substantial degradation caused by the illumination in the photosensitive samples of the Y_{L167} mutant, the spectra were recorded quickly using a scanning rate of 1800 nm/min. Each measurement was carried out using a fresh sample due to the limited reversibility of the signals. For the same reason, the dark spectra used for light-minus-dark difference spectra were taken after illumination.

EPR Spectroscopy. Light-minus-dark EPR spectra were recorded using a Bruker E580 X-band spectrometer. The magnetic field modulation frequency was 100 kHz, the amplitude was 0.4 mT, the microwave power was 10 mW, and the microwave frequency was approximately 9.64 GHz. A quartz flat cell mounted in a Bruker TE_{102} rectangular standard cavity was used to hold the samples. Each spectrum was the average of 50 scans. The sweep time was 21 s/scan, and the time constant was 82 ms. The spectra were obtained at ambient temperature.

Proton Uptake/Release Measurements. Light-induced changes in pH were determined by measuring the absorption changes of pH-sensitive dyes (bromocresol purple, for pH 5.6−7.4; *o*-cresol red, for pH 7.4−8.7, and *o*-cresolphthalein, for pH 8.6−9.6) at 586 nm (*15*). A magnetic stirrer was mounted under a cell holder of local design in order to get a rapid distribution of added buffer or acid. The net H^+ binding/release was determined at each pH value as the difference of the dye responses between the unbuffered and buffered (10 mM) samples. The following buffers were used: 2-(*N*-morpholino)ethanesulfonic acid (Mes), for pH 5.6−6.7; *N*-(2-hydroxyethyl)piperazine-*N*′-2-ethanesulfonic acid (Hepes), for pH 7.0−8.0; Tris-HCl, for pH 7.6−8.8; and 2-(*N*-cyclohexylamino)ethanesulfonic acid (Ches), for pH 8.6−9.6. To determine the buffering capacity of the entire system, a known amount of strong acid (HCl) was added during extensive stirring of the sample solution. Absorption of carbon dioxide was prevented by the use of degassed solutions and by saturating the gas phase over the samples with nitrogen gas. Terbutryn at a concentration of 100 μM was added to block interquinone electron transfer. The concentration of the photochemically active reaction centers was determined by monitoring the absorbance changes at 450 nm, the characteristic wavelength of the Q_A/Q_A^- transition.

RESULTS

A Tyrosyl Radical Is Present in the Y_{L167} and Y_M Mutants. In light-induced changes of the optical absorption spectrum, the state P^+ has a well-defined absorption band centered at 1250 nm, as seen for the quadruple mutant (Figure 2A). Both

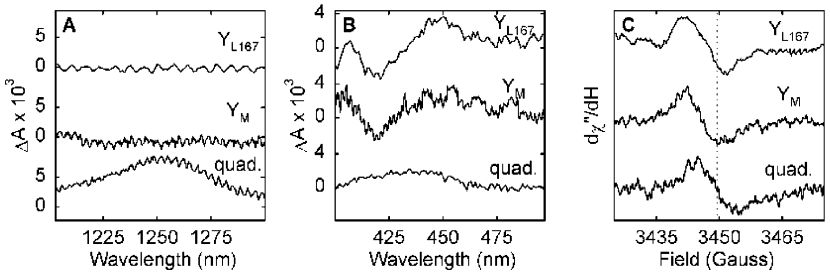

FIGURE 2: Light-minus-dark difference optical spectra of the Y_{L167}, Y_M, and quadruple mutants in the 1200−1300 nm region (A) and in the 400−500 nm region (B), and light-minus-dark difference X-band EPR spectra of mutant reaction centers (C). The EPR spectra have g values of 2.0039, 2.0045, and 2.0026 for the Y_{L167}, Y_M, and quadruple mutants, respectively. The vertical dashed line shows the position of $g = 2.0025$. Conditions: The reaction center concentration was 7 μM (A), 1.5 μM (B), and ~300 μM (C) in 0.05% Triton X-100, 1 mM EDTA, 15 mM Ches, and 100 μM terbutryn. The optical measurements were made on samples at pH 10, and the EPR measurements were made on samples at pH 9. The scanning rate for the optical measurements was 900 nm/min for the quadruple and the Y_M mutants and 1800 nm/min for the Y_{L167} mutant to avoid irreversible spectral changes in the samples.

the Y_M and Y_{L167} mutants show no optical band in this region at pH 10, demonstrating that P^+ is reduced by a secondary electron donor. The absorption changes in the 400−500 nm region measured at pH 10 are in agreement with these assignments (Figure 2B). The quadruple mutant shows a broad band attributed to the state $P^+Q_A^-$. Both the Y_M and Y_{L167} mutants show a distinctive absorption decrease centered near 420 nm. The addition of ferrocene, a spectrally silent fast exogenous donor to P^+, results in the loss of these bands, and only a small band centered at 450 nm can be seen due to Q_A^- (data not shown). The absorption decrease at 420 nm has previously been associated with formation of tyrosyl radicals in reaction center mutants (*11*). The presence of a tyrosyl radical in the Y_{L167} mutant is corroborated by a shift in the g value of the light-induced EPR signal compared to the quadruple mutant (Figure 2C). This EPR signal, taken at pH 9, is likely predominantly a tyrosyl radical with a minor contribution from P^+ (*11*, *18*).

Proton Uptake/Release Is Similar in the Y_{L167} and Quadruple Mutants. The pH-dependent stoichiometry of the light-induced proton uptake/release was measured for the Y_{L167} mutant and found to range from +0.1 to 0.3 H^+/reaction center between pH 6 and pH 10 (Figure 3). Within the error of the measurements, the light-induced protonational changes are essentially the same for the Y_{L167} mutant and the quadruple mutant, which has been measured previously to have the same pH dependence for proton uptake/release as observed for wild type (*15*). In contrast, the proton uptake/release from the Y_M mutant starts at +0.1 H^+/reaction center at pH 6 but increases to a maximal value of −0.25 at pH 8, with a completely different pH dependence from the quadruple mutant as previously described (*15*).

The Light-Induced Near-Infrared Spectrum of the Y_{L167} Mutant Is Unique. The reversible light-induced absorption changes in the 700−1000 nm region are distinctive for each of the mutants (Figure 4A). The quadruple mutant shows the same features between pH 6 and pH 11 as observed for wild type, including a bleaching of the band at 865 nm due to loss of P, a derivative signal centered near 800 nm due to electrochromic shifts of the bacteriochlorophyll monomer bands in the presence of P^+, and an electrochromic shift of the bacteriopheophytin band near 760 nm due to reduction of the quinone. The Y_M mutant above pH 8 lacks the absorption changes at 865 and 800 nm because of reduction of P^+ by Tyr M164 but retains the spectral features near 760 nm associated with Q_A^-. For the Y_{L167} mutant, the

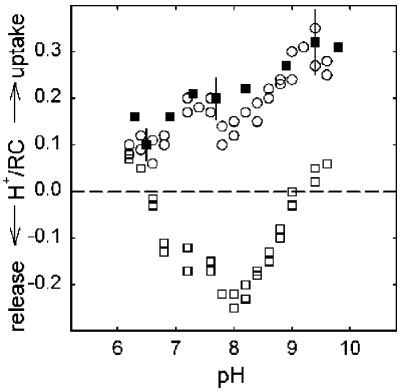

FIGURE 3: pH dependence of the light-induced proton uptake/release by reaction centers from the Y_{L167}, Y_M, and quadruple mutants. The proton uptake of the Y_{L167} mutant (filled squares) was calculated as the difference in the light-induced absorption changes of pH-sensitive dyes in the presence and absence of buffers. The proton uptake/release data by the quadruple mutant (open circles) and by the Y_M mutant (open squares) are taken from ref *15*. Conditions: 7 μM reaction centers, 0.05% Triton X-100, 100 mM NaCl, 40 μM pH indicator dye, and 10 mM buffers (when present). The dyes and the buffers with the pH ranges in which they are applicable are listed in the Materials and Methods section as well as the illumination conditions of the samples. For the Y_{L167} mutant, each data point was determined using a fresh sample.

spectrum has a negative absorption change at 875 nm, a positive change at 810 nm, and small changes at 770 and 747 nm. Under continuous light excitation, these signals reached their maximum amplitude after several seconds, and after switching off the light they decayed in approximately 2 min.

The light-induced change in the optical spectrum of the Y_{L167} mutant at pH 10 was decomposed in terms of shifts in the absorption bands of the individual chromophores of the reaction center. The ground state spectrum has bands centered at 758, 803, and 861 nm, due to absorption of the bacteriopheophytins, bacteriochlorophyll monomers, and P, respectively (Figure 4B). The widths of the absorption bands were determined by Gaussian fits of the individual bands of the optical spectrum, yielding a width at half-maximum of 30 nm centered at 861 nm for the P band, 8.6 nm centered at 809 and 794 nm for each bacteriochlorophyll monomer contribution to the 803 nm band, and 16.6 nm centered at 758 nm for both of the bacteriopheophytins. Because the shift in the bacteriopheophytin band is much smaller and mainly due to the formation of Q_A^-, that band was not decomposed into the two individual contributions for sim-

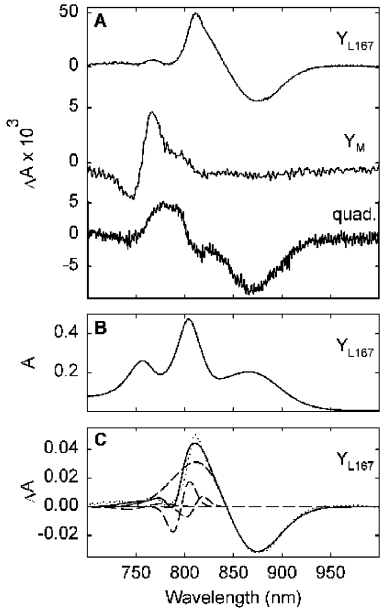

FIGURE 4: Near-infrared light-minus-dark difference spectra of the Y_{L167}, Y_M, and quadruple mutants (A), near-infrared absorption spectrum of the Y_{L167} mutant (B), and fit of the near-infrared light-induced absorption changes of the Y_{L167} mutant (C) at pH 10. The light-minus-dark spectrum of the Y_{L167} mutant was fit assuming shifts in the Q_y absorption bands of the chromophores in the reaction center. The individual contributions of the chromophores are drawn as dashed lines, and the sum of the individual contributions is shown as a solid line, while the experimental spectrum is a dotted line. The conditions of the fit are described in the text. The fit resulted in the following bandshifts: the P band from 861 to 829 nm, the monomer bacteriochlorophyll bands from 809 to 811 nm and from 794 to 799 nm, and the bacteriopheophytin bands from 758 to 759 nm. Conditions were the same as in Figure 2. The concentration of the reaction centers was 1.5 μM.

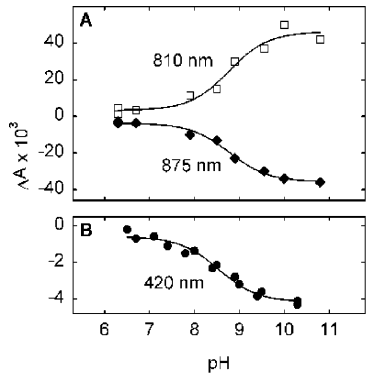

FIGURE 5: pH dependence of the optical absorption changes in the Y_{L167} mutant. The light-induced changes were measured at 875 and 810 nm (A) and at 420 nm (B) from the reversible light-minus-dark difference absorption spectra recorded at different pH values. The data at 875, 810, and 420 nm were fit with single Henderson−Hasselbalch-type equations, yielding pK_a values of 8.78 ± 0.08, 8.76 ± 0.15, and 8.54 ± 0.10, respectively. Conditions as in Figure 3 except Mes, Hepes, Tris-HCl, Ches, or a combination of these was used as the buffer (total of 15 mM) depending on the pH. Fresh samples were prepared at each pH value.

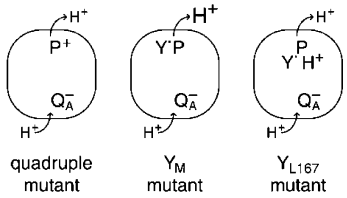

FIGURE 6: Schematic comparison of the quadruple, Y_M, and Y_{L167} mutants. In response to light, the $P^+Q_A^-$ state is formed in the quadruple mutant, and the $Y^\bullet Q_A^-$ state is formed in the Y_M and Y_{L167} mutants. Compared to the quadruple mutant, the Y_M mutant has a significantly larger proton release. The magnitude of the proton release in the Y_{L167} mutant is similar to that of the quadruple mutant, indicating the trapping of the phenolic proton of the tyrosine in the protein in the close vicinity of P. Proton uptake by Q_A^- is assumed to be comparable in all three cases.

plicity. Making use of these individual assignments, a fit of the light-induced spectrum yielded a shift of the P band to the blue from 861 to 829 nm, shifts of the bacteriochlorophyll monomer bands from 809 to 811 nm and from 794 to 799 nm, and a shift of the bacteriopheophytin band to the red by 1 nm from 758 to 759 nm (Figure 4C).

Dependence of the Yield of Tyrosine Oxidation in the Y_{L167} Mutant on pH. The relative amount of P^+Y formed compared to the amount of $PY^\bullet$ is observed to be highly pH dependent in the Y_M mutant, with the tyrosyl radical state being favored at high pH rather than the P^+Y state (*11*, *18*). This is attributable to the requirement for the formation of a tyrosyl radical that the phenolic proton be released upon oxidation. At pH 10 the amount of P^+ observed in the light-induced optical spectrum of the Y_{L167} mutant (Figure 2A) was minimal, indicating that the yield of tyrosyl radical formation was close to unity at this pH under the conditions used. Each of the absorption changes measured at the characteristic wavelengths of 875, 810, and 420 nm followed the same pH-dependent pattern. The amplitude of the electrochromic optical absorption changes in the 700−1000 nm region (Figure 4) increased approximately 10-fold as the pH increased from 6.3 to 10.0 in the Y_{L167} mutant with no additional changes above pH 10 (Figure 5A). Similarly, the signal at 420 nm, identified previously as a measure of tyrosine oxidation (*11*, *18*), increased approximately 8-fold in the same pH range and reached a maximal value at pH 10 (Figure 5B). Fitting the absorption changes with a Henderson−Hasselbalch equation yielded pK_a values of 8.78 ± 0.08, 8.76 ± 0.15, and 8.54 ± 0.10 for the data at 875, 810, and 420 nm, respectively. Thus, the yield of the tyrosyl state of the Y_{L167} mutant was highly pH dependent, with a pK_a of approximately 8.7 and a maximal value above pH 10. The Y_{L167} mutant shows a shift in the *g* value of the EPR spectrum compared to the quadruple mutant at pH 9, indicating the presence of the tyrosyl radical (Figure 2C). Quantification of the pH dependence of the EPR spectrum measured at room temperature was not performed because of preferential accumulation of the tyrosyl radical due to the shorter lifetime of P^+ compared to $Y^\bullet$ under the conditions used for the EPR measurements. In addition, quantification of the EPR spectrum is hampered by the lack of detectable hyperfine coupling due to the poor signal-to-noise ratio in the room temperature measurements.

DISCUSSION

The Y_{L167} mutant was found to have some characteristics that resemble those of the Y_M mutant, which has been shown to produce a tyrosyl radical at M164, and some characteristics that resemble those of the quadruple mutant, which does not form a tyrosyl radical (Figure 6). Spectral signatures indicating the loss of P^+ and the appearance of a tyrosyl radical in the Y_{L167} mutant show that the tyrosine residue introduced

at L167 is oxidized by P^+, as is the tyrosine residue at M164 in the Y_M mutant. Unlike the Y_M mutant, tyrosyl formation in the Y_{L167} mutant does not lead to a large increase in the relative amount of released proton, and the proton uptake/release in the Y_{L167} mutant is comparable to that in the quadruple mutant. A clue to the resolution of this apparent incongruity in the Y_{L167} mutant is found in the near-infrared optical spectrum, which can be interpreted as being electrostatically altered by a nearby charged species. Thus the results support a model in which the phenolic proton from the oxidized tyrosine at L167 is trapped in the protein rather than being released to the bulk as occurs for the Y_M mutant. The evidence for this model and the relationship between the spectral changes and the proton release in these mutants as well as other proteins are discussed.

Since the only difference between the quadruple mutant and the Y_{L167} mutant is the tyrosine introduced at L167, differences between these two mutants must arise from the introduction of the tyrosine. In the quadruple mutant, light excitation forms the charge-separated state $P^+Q_A^-$ when electron transfer to Q_B is blocked, as confirmed by the light-induced spectral changes. The $P^+Q_A^-/PQ_A$ difference spectrum of the quadruple mutant has the same shape and amplitude at every pH value. The spectral shape is identical with that measured in wild type, but due to the low quantum yield of this mutant the amplitudes are decreased to 5−10% of wild type. The light-induced optical spectrum of the Y_{L167} mutant shows the electrochromic shift of the bacteriopheophytins in the 750 nm region, indicating the presence of Q_A^-, but other spectral features are distinctive from those of the quadruple mutant and are similar to those of the Y_M mutant. The lack of spectral features of P^+ such as the optical band at 1250 nm indicates the presence of an internal secondary donor. The absorption decrease at 420 nm and the shift in the *g* value of the light-induced EPR spectrum are consistent with tyrosine being the identity of the secondary donor. These features are associated specifically with the tyrosine replacement at Phe L167, as a leucine substitution at this position resulted in only relatively minor changes in the characteristics of the reaction center (*19*).

The net proton uptake for this mutant was found to be the same within the experimental error as was determined for the quadruple mutant (Figure 3). In the quadruple mutant, as in wild type, the light-induced protonational changes are based on electrostatic interactions and have contributions from both Q_A^- (uptake) and P^+ (release). Since no changes were made at the acceptor side of the reaction centers, the proton uptake associated with the Q_A^- formation should be the same in all three mutants (*15*). In the Y_{L167} mutant, as the pH was raised, the yield of tyrosyl radical formation increased and reached a maximum at pH 10 (Figure 5). Therefore, at approximately pH 10 the proton release is almost exclusively due to the presence of the tyrosyl radical, since P^+ is not detectable at this pH (Figure 2A). The similarity of the net proton uptake at high pH values implies that the electrostatic proton release associated with the formation of P^+ in the quadruple mutant is approximately equal to the proton release induced by oxidation of Tyr L167 in the Y_{L167} mutant. The proton release associated with the oxidation of the L167 Tyr is likely to be similarly of electrostatic origin. The similarity in the protonational changes between the quadruple and Y_{L167} mutant is consistent with a positive charge remaining localized near P in the Y_{L167} mutant.

An electrostatic interaction in the Y_{L167} mutant is indicated by the modeling of the near-infrared light-induced spectrum as a substantial 32 nm blue shift of P and a smaller red shift in the bands of the monomer bacteriochlorophylls. The shift in the bacteriopheophytin band is present in the spectra of each of the three reaction center mutants and arises from the reduction of the primary quinone (*20*). The 32 nm blue shift of the P band corresponds to a 50 meV increase in the energy difference between the ground and excited states of P. Theoretical calculations have predicted significant shifts of the Q_y absorption bands of the bacteriochlorophylls if point charges are placed in the close vicinity of the tetrapyrrole rings (*21*). According to these calculations, the magnitude and direction of the optical shifts will depend on both the placement of the point charge relative to the tetrapyrrole and the sign of the point charge. Positive charges placed near rings C and E or negative charges situated near ring A are predicted to cause blue shifts whereas reversing the charges should result in red shifts. Thus, the localization of a proton near Tyr L167 would place a positive charge approximately 5 Å from ring E on the L side of P (Figure 1) and is predicted to result in a significant blue shift as is observed. The shifts on the bacteriochlorophyll monomer bands are much smaller, probably corresponding to the larger distance of 10 Å between the putative charge and these chromophores. It is also possible that the blue shift of the dimer band is due to a structural change upon oxidation of Tyr L167. Blue shifts of the absorption band of the dimer have been observed in reaction centers with mutations at L167 and L168 (*19*).

A proton release of 0.5 $H^+/Y^{\bullet}_{M164}$ to the bulk solvent phase is associated with oxidation of Tyr M164 in the Y_M mutant, after subtraction of the contribution of Q_A^- (*15*). No signs of electrochromic bandshifts in the absorption bands of the bacteriochlorophylls in the near-infrared region were observed in the spectrum of the Y_M mutant, which showed only features characteristic of a Q_A^-/Q_A difference spectrum (*11*, *18*). It should be noted that the reduction of the quinone also causes small shifts in the Q_y absorption bands of the dimer and the monomeric bacteriochlorophylls, but these absorption changes are negligible due to the large distance of over 20 Å between Q_A^- and the bacteriochlorins (*20*).

The measured proton release in the Y_M mutant could proceed either through a direct proton transfer pathway or through electrostatic interactions (15). On the basis of the results for the Y_{L167} mutant, if the proton transfer from Tyr M164 occurs via electrostatic interactions, then even with a larger distance of 10 Å between M164 and P compared to 5 Å between L167 and P, a distinctive electrochromic shift of the 865 nm optical absorption band should be evident. However, no measurable shifts are observed in any of the optical bands in the Y_M mutant. Thus, proton transfer from Tyr M164 in the Y_M mutant probably occurs by direct proton transfer involving His M193 and Glu M173.

Large electrochromic shifts of the optical spectrum were found only for the Y_{L167} mutant, which has a limited proton release upon tyrosyl formation. In this mutant, the phenolic proton of Tyr L167 may be transferred upon oxidation to a nearby acceptor but not subsequently released to the bulk. This would result in the presence of a positive charge near the bacteriochlorophylls, with the consequent electrochromic

shifts. If the phenolic proton is released to the bulk, as found in the Y_M mutant, the positive charge would not be retained in the protein, and no electrochromic shifts would occur.

The pH dependence of the optical spectrum of the Y_{L167} mutant emphasizes the importance of the protein environment for tyrosyl radicals, particularly the identity of the residue serving as the acceptor of the phenolic proton of the tyrosine. Proton transfer makes tyrosine oxidation energetically feasible by substantially reducing the midpoint potential of the tyrosine by several hundred millivolts (*12*−*14*). In the Y_{L167} mutant, the amplitude of the electrochromic absorption changes exhibited a strong pH dependence, increasing 10-fold between pH 6.3 and pH 10.0. The amplitude of the signal at 420 nm, an optical measure of the tyrosine oxidation, showed a similar pH-dependent pattern (Figure 5). The pH dependencies of these signals had similar pK_a values, indicating that they probably arise from the same phenomenon. One explanation for this dependence is that a nearby residue, such as Cys L247, becomes deprotonated at high pH, allowing it to serve as a proton acceptor for the phenolic proton. One difference observed for the Y_{L167} mutant compared to the Y_M mutant is that the optical signals that correspond to P^+ do not appear at lower pH values, although the signal associated with the tyrosine and the electrochromic shifts both decrease in amplitude. A scheme in which at low pH another species becomes rapidly oxidized by the tyrosyl radical whereas at high pH the tyrosyl radical is stable could account for the pH-dependent behavior.

Differences in the local protein environments are likely responsible for the large proton release for Tyr M164 compared to Tyr L167. In wild-type reaction centers, Arg M164 is only approximately 5 Å from the protein surface, while Phe L167 is much further at approximately 10 Å from the surface. Assuming that they are positioned similarly to the native residue and allowing for limited movement within the existing pocket, neither Tyr M164 nor Tyr L167 would be exposed to the surface in the Y_M and Y_{L167} mutants, respectively, and Tyr M164 would be closer to the surface and further from P than Tyr L167. A potential proton-conducting pathway that can deliver the phenolic proton to the bulk is evident for Tyr M164 (Figure 1). His M193, the putative proton acceptor for Tyr M164 (*11*, *18*), is modeled to be within hydrogen-bonding distance to Tyr M164. Glu M173, which is largely exposed on the surface, is also modeled to be within 5 Å of Tyr M164 and within hydrogen-bonding distance to His M193. Thus the relatively short pathway Tyr M164−His M193−Glu M173 leads to the surface. In contrast, Tyr L167 is located in a largely hydrophobic region of the protein with no chain of protonatable residues evident for transfer of the proton to the bulk (Figure 1). The closest residues to the hydroxyl group of Tyr L167 would be Cys L247, Met L248, and Thr L251. Of these three residues, only Cys L247, which is approximately 5 Å from P, could act as a proton acceptor. Cys L247 and Met L248 have no obvious interactions with nearby residues, while Thr L251 forms hydrogen bonds with Asn L170 and Trp L259 in the wild type. Residues near the ring of L167 include Gly L161, Tyr L164, Asn L170, and Trp L259. In addition, a large part of the pocket around L167 is formed by one of the bacteriochlorophylls of P, which is approximately planar with Phe L167. The closest surface residues, such as Thr L163, are approximately 10 Å from L167. The more hydrophobic milieu of Tyr L167 also suggests a lower dielectric constant and thus stronger electrostatic interactions as compared to the more hydrophilic surroundings of Tyr M164.

It has been reported by many groups that tyrosine oxidation in photosystem II is pH dependent (*22*−*24*) and is accompanied by shifts of the absorption bands of nearby tetrapyrroles (*25*−*31*). However, these shifts in the near-infrared region are only a few nanometers compared to the 32 nm shift reported for the Y_{L167} mutant, indicating a much weaker electrostatic interaction. The lack of a large electrochromic shift in photosystem II indicates that the proton from $Y_Z^{\bullet}$ is not trapped within 5 Å of the chromophores. On the other hand, the small shift can give some clue to the fate of the proton, because if it were completely dispersed, there would be no shift. The extent of the electrochromic shift depends on several factors that influence electrostatic interactions (*32*), such as the distance, dielectric constant, and distribution of the proton, which remain unknown in photosystem II. The electrostatic interactions determined for the Y_{L167} mutant also have implications for other proteins containing amino acid radicals, as in many systems the close distance between the radical and the active site, of 3−5 Å, would imply a strong electrostatic interaction if the proton associated with the radical is not transferred away from the site.

ACKNOWLEDGMENT

We thank C. Magee for cell growth and reaction center preparation and B. Bowen for help with the data analysis.

REFERENCES

1. Blankenship, R. E., Madigan, M. T., and Bauer, C E., Eds. (1995) *Anoxygenic Photosynthetic Bacteria*, Kluwer Academic Publishers, Dordrecht, The Netherlands.
2. Heathcote, P., Fyfe, P. K., and Jones, M. R. (2002) *Trends Biochem. Sci. 27*, 79−87.
3. Maróti, P., and Wraight, C. A. (1988) *Biochim. Biophys. Acta 934*, 329−347.
4. McPherson, P. H., Okamura, M. Y., and Feher, G. (1988) *Biochim. Biophys. Acta 934*, 348−368.
5. Allen, J. P., Feher, G., Yeates, T. O., Komiya, H., and Rees, D. C. (1987) *Proc. Natl. Acad. Sci. U.S.A. 84*, 6162−6166.
6. Zouni, A., Witt, H. T., Kern, J., Fromme, P., Krauss, N., Saenger, W., and Orth, P. (2001) *Nature 409*, 739−743.
7. Debus, R. J., Barry, B. A., Sithole, I., Babcock, G. T., and McIntosh, L. (1988) *Biochemistry 27*, 9071−9074.
8. Metz, J. G., Nixon, P. J., Rogner, M., Brudvig, G. W., and Diner, B. A. (1989) *Biochemistry 28*, 6960−6969.
9. Debus, R. J., Barry, B. A., Babcock, G. T., and McIntosh, L. (1988) *Proc. Natl. Acad. Sci. U.S.A. 85*, 427−530.
10. Vermaas, W. F. J., Rutherford, A. W., and Hansson, O. (1988) *Proc. Natl. Acad. Sci. U.S.A. 85*, 8477−8481.
11. Kálmán, L., LoBrutto, R., Allen, J. P., and Williams, J. C. (1999) *Nature 402*, 696−699.
12. Tommos, C., and Babcock, G. T. (2000) *Biochim. Biophys. Acta 1458*, 199−219.
13. Diner, B. A. (2001) *Biochim. Biophys. Acta 1503*, 147−163.
14. Debus, R. J. (2001) *Biochim. Biophys. Acta 1503*, 164−186.
15. Kálmán, L., Williams, J. C., and Allen, J. P. (2003) *FEBS Lett. 545*, 193−198.
16. Williams, J. C., Alden, R. G., Coryell, V. H., Lin, X., Murchison, H. A., Peloquin, J. M., Woodbury, N. W., and Allen, J. P. (1992) in *Research in Photosynthesis* (Murata, N., Ed.) Vol. I, pp 377−380, Kluwer Academic Publishers, Dordrecht, The Netherlands.

17. Lin, X., Murchison, H. A., Nagarajan, V., Parson, W. W., Allen, J. P., and Williams, J. C. (1994) *Proc. Natl. Acad. Sci. U.S.A. 91*, 10265−10269.
18. Narváez, A. J., Kálmán, L., LoBrutto, R., Allen, J. P., and Williams, J. C. (2002) *Biochemistry 41*, 15253−15258.
19. Murchison, H. A., Alden, R. G., Allen, J. P., Peloquin, J. M., Taguchi, A. K. W., Woodbury, N. W., and Williams, J. C. (1993) *Biochemistry 32*, 3498−3505.
20. Verméglio, A., and Clayton, R. K. (1977) *Biochim. Biophys. Acta 461*, 159−165.
21. Hanson, L. K., Thompson, M. A., Zerner, M. C., and Fajer, J. (1989) in *The Photosynthetic Bacterial Reaction Center I* (Breton, J., and Verméglio, A., Eds.) pp 355−367, Plenum Press, NATO ASIS Publishers, New York.
22. Gilchrist, M. L., Ball, J. A., Randall, D. W., and Britt, R. D. (1995) *Proc. Natl. Acad. Sci. U.S.A. 92*, 9545−9549.
23. Hays, A.-M. A., Vassiliev, I. R., Golbeck, J. H., and Debus, R. J. (1999) *Biochemistry 38*, 11851−11865.
24. Vass, I., and Styring, S. (1991) *Biochemistry 30*, 830−839.
25. Dekker, J. P., Van Gorkom, H. J., Brok, M., and Ouwehand, L. (1984) *Biochim. Biophys. Acta 764*, 301−309.
26. Diner, B. A., and De Vitry, C. (1984) in *Advances in Photosynthesis Research* (Sybesma, C., Ed.) Vol. I, pp 407−411, Martinus Nijhoff/Dr. W. Junk Publishers, The Hague, The Netherlands.
27. Diner, B. A., Tang, X.-S., Zheng, M., Dismukes, G. C., Force, D. A., Randall, D. W., and Britt, R. D. (1995) in *Photosynthesis: From Light to Biosphere* (Mathis, P., Ed.) Vol. II, pp 229−234, Kluwer Academic Publishers, Dordrecht, The Netherlands.
28. Haumann, M., and Junge, W. (1996) in *Oxygenic Photosynthesis: The Light Reactions* (Ort, D. R., and Yocum, C. F., Eds.) pp 165−192, Kluwer Academic Publishers, Dordrecht, The Netherlands.
29. Mulkidjanian, A. Y., Cherepanov, D. A., Haumann, M., and Junge, W. (1996) *Biochemistry 35*, 3093−3107.
30. Rappaport, F., Blanchard-Desce, M., and Lavergne, J. (1994) *Biochim. Biophys. Acta 1184*, 178−192.
31. Diner, B. A., Schlodder, E., Nixon, P. J., Coleman, W. J., Rappaport, F., Lavergne, J., Vermaas, W. F. J., and Chisholm, D. A. (2001) *Biochemistry 40*, 9265−9281.
32. Johnson, E. T., and Parson, W. W. (2002) *Biochemistry 41*, 6483−6494.

BI034970L